

# Thermodynamic Properties of Transition Metals Using Face-Centered-Cubic Lattice Model with Renormalized Potentials

Ryoji Sahara<sup>1,\*</sup>, Hiroshi Mizuseki<sup>1</sup>, Kaoru Ohno<sup>2</sup> and Yoshiyuki Kawazoe<sup>1</sup>

<sup>1</sup>Institute for Materials Research, Tohoku University, Sendai 980-8577, Japan

<sup>2</sup>Department of Physics, Graduate School of Engineering, Yokohama National University, Yokohama 240-8501, Japan

The thermodynamic properties of transition metals are studied by introducing face-centered cubic (FCC) lattice model. In order to treat actual systems as quantitatively as possible, empirical second moment approximation (SMA) potentials proposed by Rosato *et al.* and by Cleri *et al.*, which have been used widely for molecular dynamics (MD) simulations, are employed. To overcome shortcomings of lattice-gas models such as neglecting internal entropy of the system, the potential is mapped onto FCC lattice using the renormalization technique. It is found that the computed linear thermal expansion coefficients agree well with the results of MD simulations.

(Received January 14, 2005; Accepted March 8, 2005; Published June 15, 2005)

**Keywords:** transition metal, lattice-gas model, thermal expansion, renormalization, potential renormalization, molecular dynamics

## 1. Introduction

Lattice models are a simple and fast method for the study of thermodynamic properties. One advantage is that it can treat systems larger both in time scale and in spatial size as compared with atomic-scale molecular dynamics (MD) simulations so that it can treat qualitatively thermodynamic equilibrium or diffusion phase transition phenomena in the solid state. Although it has been pointed out<sup>1)</sup> that thermal lattice vibrations (anharmonicity effects) play an essential role, its effect has not yet been properly treated in the lattice model. Masuda-Jindo *et al.* studied the thermal properties of transition metals using an analytic statistical moment method.<sup>2)</sup> They showed that including explicitly the anharmonic effects of the lattice vibrations gives highly accurate thermodynamic quantities.

To overcome the problem of neglecting the internal entropy which originates from thermal vibrations, the potential renormalization technique proposed by one of us<sup>3,4)</sup> has been used. It offers an effective way to map interatomic potentials (for example, classical MD potentials) onto lattice models.

In previous papers,<sup>5,6)</sup> we have tried to reproduce the solid-liquid phase transition in Si using MC simulation on the basis of a body-centered-cubic (BCC) lattice model by renormalizing an empirical potential proposed by Tersoff.<sup>7)</sup> Many improvements were found when the renormalized Tersoff potential was used compared with using the original Tersoff potential directly on the BCC lattice.

The technique was also applied to an FCC lattice model to investigate the order-disorder phase transition phenomena in Cu–Au alloys.<sup>8,9)</sup> In that study, a Finnis–Sinclair-type potential<sup>10)</sup> by Ackland *et al.*<sup>11,12)</sup> and slightly refined later by Deng *et al.*<sup>13)</sup> was introduced. It was shown that the computed phase diagram agrees better with experiment when the potential renormalization technique is applied on the FCC lattice. We note that the present analytic scheme is a powerful tool when we combine it with lattice Monte Carlo simulations.

In the present study, the thermodynamic properties such as the thermal expansion coefficient of transition metals and noble metals are estimated with a FCC lattice model potential renormalization of second moment approximation (SMA) tight-binding (TB) potentials.<sup>14,15)</sup> Two sets of SMA parameters have been used; The first is proposed by Rosato *et al.*<sup>16)</sup> whose cut-off radius is restricted to the first neighbors, and the second is proposed by Cleri *et al.*<sup>17)</sup> whose cut-off radius is extended to the fifth neighbors. The results are compared with the previous-in principle exact-MD simulations<sup>16,17)</sup> and experimental results<sup>18)</sup> when available.

## 2. Model

### 2.1 Potential function

To estimate the thermodynamic properties of FCC transition metals, we use SMA–TB potentials. The potential can treat transition metals whose cohesive properties originate from the large  $d$ -band density of states, and is based on a small set of adjustable parameters and is suitable for extension to higher-order approximation through considering higher moments of the electron density of states (DOS).<sup>14,15)</sup>

In the potential, the band energy can be written for an atom  $i$  as

$$E_b^i = - \left\{ \sum_j \xi^2 \exp \left[ -2q \left( \frac{r_{ij}}{r_0} \right) - 1 \right] \right\}^{1/2}, \quad (1)$$

where  $\xi$  is an effective hopping integral,  $r_{ij}$  is the distance between atoms  $i$  and  $j$ , and  $r_0$  is the first-neighbor distance that gives  $r_0 = a_0/\sqrt{2}$  with the correct atomic volume  $\Omega_0 = a_0^3/4$ . The parameter  $q$  describes the distance dependence of the hopping integral.

To ensure stability of the system, a repulsive pairwise interaction of Born–Mayer type is added:

$$E_r^i = \sum_j A \exp \left[ -p \left( \frac{r_{ij}}{r_0} - 1 \right) \right] \quad (2)$$

the total cohesive energy is then given by

\*Corresponding author, E-mail: sahara@imr.edu

Table 1 Parameters of the Rosato potential<sup>(1)</sup> and Cleri potential<sup>(2)</sup>.

	$A$ (eV)	$\xi$ (eV)	$p$	$q$	$a_0$ (nm)
Ni <sup>(1)</sup>	0.1368	1.756	10.00	2.70	0.352
Cu <sup>(1)</sup>	0.0993	1.354	10.08	2.56	0.361
Rh <sup>(1)</sup>	0.0969	1.996	14.92	2.51	0.380
Pd <sup>(1)</sup>	0.1681	1.720	10.84	3.67	0.389
Ag <sup>(1)</sup>	0.1232	1.281	10.12	3.37	0.409
Ir <sup>(1)</sup>	0.144	2.499	14.53	2.90	0.384
Pt <sup>(1)</sup>	0.2341	2.503	10.80	3.50	0.392
Ni <sup>(2)</sup>	0.0376	1.070	16.999	1.189	0.3523
Cu <sup>(2)</sup>	0.0855	1.224	10.960	2.278	0.3615

(1) parameters from Ref. 16)

(2) parameters from Ref. 17)

$$E_c = - \sum_c (E_b^i + E_r^i). \quad (3)$$

The parameters  $A$ ,  $\xi$ ,  $p$ , and  $q$  are determined by fitting the experimental values of cohesive energy, lattice parameter, and bulk modulus.

In the present study, 7 FCC metals (Ni, Cu, Rh, Pd, Ag, Ir, and Pt) are studied using a set of parameters proposed by Rosato *et al.* (Hereafter, Rosato potential).<sup>16)</sup> In the Rosato potential, the summation over  $j$  in eqs. (1) and (2) are restricted to the first neighbors, which is suitable for the potential renormalization scheme. To check the effect of the cut-off radius of the potential parameters into the potential renormalization scheme, another parameter set proposed by Cleri *et al.* whose cut-off radius is extended to 5th neighbors (Cleri potential)<sup>17)</sup> is also introduced for Ni and Cu.

Note that although it is known that the SMA for the  $d$  band is well suited to transition metals only (it is harder to justify for noble metals where the  $d$  band is full), Rosato *et al.*, proposed the use of the same model for the noble metals from an empirical point of view.

Table 1 gives the values of  $A$ ,  $\xi$ ,  $p$ ,  $q$ , and  $a_0$  of Rosato potential and Cleri potential for all the metals studied in the present paper.

## 2.2 Potential renormalization

To apply Rosato potential and Cleri potential on FCC lattice, we use the potential renormalization technique. Since the basic ideas of the potential renormalization have been amply shown in Refs. 3–6, 8, 9 only essential points necessary for the present study are summarized.

The fundamental idea of potential renormalization is to make a new potential function for discretized space without changing the value of the partition function for continuous space. Consider that  $N$ -atom system in the continuous space with the original potential  $U(\vec{x}_1, \vec{x}_2, \dots, \vec{x}_N)$  is decomposed into  $M$  lattice sites. The configurational term of partition function is expressed as follows;

$$\begin{aligned} & \frac{1}{N!} \int d\vec{x}_1 \int d\vec{x}_2 \dots \int d\vec{x}_N \exp\left(-\frac{U(\vec{x}_1, \vec{x}_2, \dots, \vec{x}_N)}{k_B T}\right) \\ &= \frac{(M\Omega)^N}{N!} \sum_{i_1} \sum_{i_2} \dots \sum_{i_N} \exp\left(-\frac{F(i_1, i_2, \dots, i_N)}{k_B T}\right), \quad (4) \end{aligned}$$

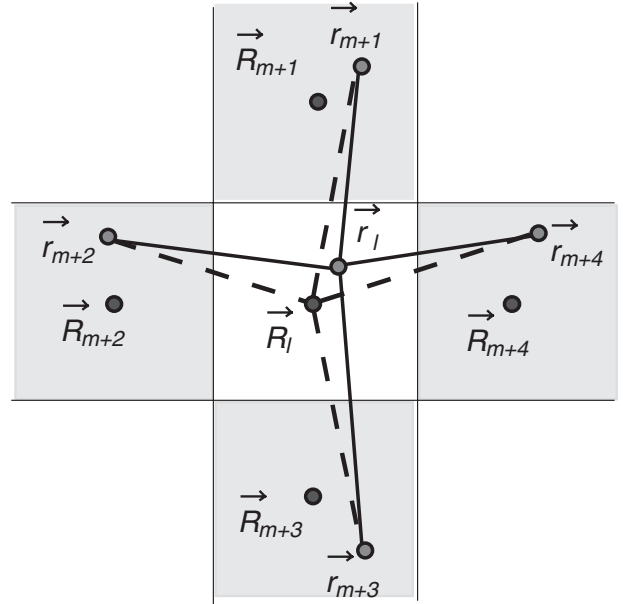


Fig. 1 Illustration of the potential renormalization scheme. Division of the configurational space is shown for the case of a 2-dimensional simple square lattice. White-colored cell is A WS cell and gray-colored cell is B WS cell. Solid lines represent the original (MD) potential and broken lines represent the desired renormalized potential.

where,  $\Omega$  is the volume of one lattice site,  $i_k$  runs over all the  $M$  lattice sites, and  $F(i_1, i_2, \dots, i_N)$  is the desired renormalized potential which is determined by a knowledge of the original MD potential. Here, how to use this technique in the case of FCC metals is explained. Since four sublattices are needed for an FCC lattice so as to exclude  $A$ - $A$  type nearest neighbors, one might use a “four-sublattice, four-step renormalization” technique for complete study. However, in order to reduce a large amount of the calculations, a two-sublattice, two-step renormalization technique is used here.

Consider a case where  $l$ th atom is surrounded by  $n$  atoms located in adjacent and different Wigner-Seitz (WS)-cells numbered as  $m+1, m+2, \dots, m+n$ . Figure 1 illustrates a two-dimensional square lattice in which the WS cell is given by a unit square. WS cell is decomposed into two sublattices, and we call white-colored WS cell A cell and gray-colored WS cell B cell. In this situation, only gray-colored B cells are neighbors of an white-colored A cell and vice versa. When the cut-off radius of the original potential is short, one may assume that the cut-off length of the renormalized potential to be the same order or shorter than the lattice constant so that one atom in the A WS cell is affected only by the ones in the nearest neighbor B cells. (The situation is well realized in the case of Rosato potential).

We also assume that the  $n$  coordinated atoms are surrounded further by similar configurations. Solid lines in Fig. 1 represent the original potential and broken lines represent the renormalized potential which is evaluated as follows:

In the first step of the renormalization, the trace of the  $l$ th A cell is evaluated. In other words, the renormalized potential function  $f(\vec{r}_{m+1}, \vec{r}_{m+2}, \dots, \vec{r}_{m+n})$ , which is a function of the atomic positions  $\vec{r}_{m+i}$  ( $i = 1 \sim n$ ) in the adjacent B cells, is determined by evaluating the integral of the configurational

exponential (Boltzmann factor) with respect to the atomic position  $\vec{r}_l$  inside the  $l$ th  $A$  cell, and is given as follows:

$$\exp(-\beta f(\vec{r}_{m+1}, \vec{r}_{m+2}, \dots, \vec{r}_{m+n})) = \frac{1}{\Omega_l} \int d\vec{r}_l \exp[-\beta V(\vec{r}_l; (\vec{r}_{m+1}, \dots, \vec{r}_{m+n}))], \quad (5)$$

where  $V(\vec{r}_l; (\vec{r}_{m+1}, \dots, \vec{r}_{m+n}))$  expresses the original potential,  $\beta = 1/k_B T$  reciprocal temperature, and  $\Omega_l$  volume of  $l$ th WS cell. Here, the left-hand side of (3) is decomposed into the product of functions, each of which depends only on one position, *e.g.*  $\vec{r}_{m+i}$ , only. That is, the following parameterization is introduced:

$$f(\vec{r}_{m+1}, \vec{r}_{m+2}, \dots, \vec{r}_{m+n}) = f^{(n)}(|\vec{r}_{m+1}|) + f^{(n)}(|\vec{r}_{m+2}|) + \dots + f^{(n)}(|\vec{r}_{m+n}|). \quad (6)$$

In order to reduce the large amount of calculation, further approximation is introduced. That is, when the dependence on the atomic position in the  $(m + m')$ th  $B$  cell is estimated, other atomic positions in the  $(m + m'')$ th  $B$  cells ( $m' \neq m''$ ) are fixed at the center of the cell,  $\vec{R}_{(m+m'')}$ .

The second step of the renormalization is to evaluate the trace of the  $m$ th  $B$  cell. From the first step, the renormalized potential function  $f^{(n)}(\vec{r}_{m+i})$  has already been estimated. As a result of this step, the desired renormalized potential  $F^{(n)}$  for the  $n$  coordinated configuration can be determined as follows:

$$\exp(-\beta n F^{(n)}) = \frac{1}{\Omega_m} \int d\vec{r}_m \exp\left[-\beta \left(\sum_{i=1}^n f^{(n)}(\vec{r}_m)\right)\right], \quad (7)$$

where  $\Omega_m$  is the volume of the  $m$ th WS cell, and  $nF^{(n)}$  in the left-hand side is the renormalized potential for the  $n$  coordinated configuration.

Along with the above formulation, the renormalized Rosato and Cleri potential are evaluated. To calculate the  $\vec{r}_l$ -integrals in (5) and (7), a WS cell is subdivided into 1,719 grid points.

### 3. Results and Discussion

At first, the lattice constants are estimated as a function of temperature by minimizing the renormalized potential (on-site free energy). As examples, Figs. 2(a) and (b) are the results for Ni and Cu with Rosato potential, respectively. These figures show that the lattice constant increases monotonically with the temperature.

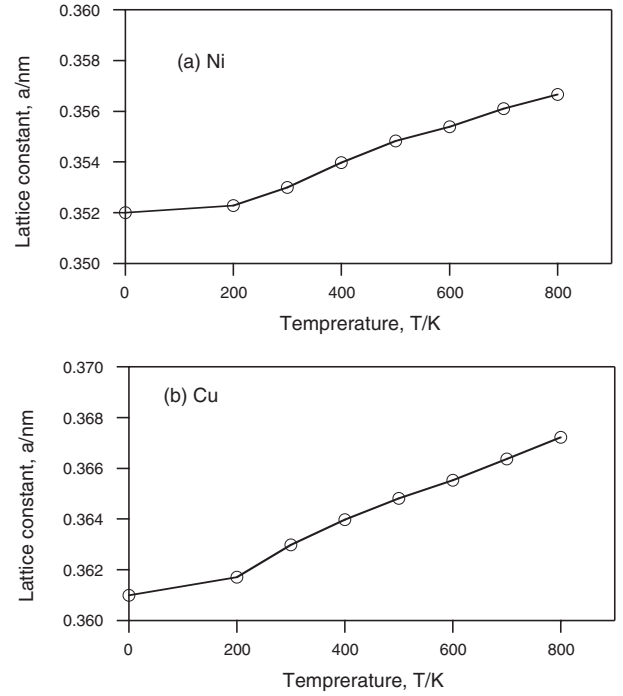


Fig. 2 Lattice constants from the potential renormalization of the Rosato potential as a function of temperature; (a) Ni and (b) Cu.

From the Figures, the linear thermal expansion coefficients,  $\alpha$ , are estimated. We obtained  $\alpha$  by averaging in the temperature range of  $0 \leq T \leq 1000$  K. We obtained  $\alpha$  of  $1.6 \times 10^{-5}$  and  $2.2 \times 10^{-5}$  for Ni and Cu, respectively. These values are in agreement with molecular dynamics simulation results performed by Rosato *et al.* of  $1.7 \times 10^{-5}$  and  $2.4 \times 10^{-5}$ <sup>16)</sup> in the temperature range of  $0.17 < T/T_m < 0.9$  with  $T_m$  is the experimental melting temperature, and also mean experimental values of  $1.53 \times 10^{-5}$  and  $1.89 \times 10^{-5}$ <sup>18)</sup> in the same temperature regions as the present simulations.

The lattice constant at 0 K,  $a_0$ , and the cohesive energy at 0 K,  $E_c$  are also estimated. Again, we obtained  $r_0$  of 0.352 and 0.361 nm for Ni and Cu, and  $E_c$  of  $-4.44$  and  $-3.50$  eV for Ni and Cu, respectively. These values reproduce exactly the original potential presented in Ref. 16).

The renormalization techniques incorporates the anharmonic term of the original SMA potential function.

We listed the values of  $\alpha$ ,  $a_0$ , and  $E_c$  for 7 FCC metals as computed with the Rosato potential in Table 2. For compar-

Table 2 Thermal lattice expansion coefficient, the lattice constant at 0 K, and the cohesive energy with Rosato potential.

	Thermal lattice expansion coefficient, $\alpha \times 10^5$			$a_0$ (nm)		$E_c$ (eV atom <sup>-1</sup> )	
	Present work	MD result <sup>16)</sup>	Experimental result <sup>18)</sup>	Present work	MD result <sup>16)</sup>	Present work	MD result <sup>16)</sup>
Ni	1.6	1.7	1.53	0.352	0.352	-4.44	-4.44
Cu	2.2	2.4	1.89	0.361	0.361	-3.50	-3.50
Rh	0.88		0.96	0.380	0.380	-5.75	-5.75
Pd	1.8		1.35	0.389	0.389	-3.94	-3.94
Ag	2.7		2.17	0.409	0.409	-2.96	-2.96
Ir	0.73		0.77	0.384	0.384	-6.93	-6.93
Pt	1.1		0.97	0.392	0.392	-5.86	-5.86

Table 3 Thermal lattice expansion coefficient, the lattice constant at 0 K, and the cohesive energy with Cleri potential.

	Thermal lattice expansion coefficient, $\alpha \times 10^5$			$a_0$ (nm)		$E_c$ (eV atom <sup>-1</sup> )	
	Present work	MD result <sup>17)</sup>	Experimental result <sup>18)</sup>	Present work	MD result <sup>17)</sup>	Present work	MD result <sup>17)</sup>
Ni	3.6	1.4	1.53	0.365	0.352	-3.31	-4.44
Cu	2.4	2.1	1.89	0.368	0.362	-3.23	-3.54

ison, the MD simulation results by Rosato *et al.* and experimental values<sup>18)</sup> are also shown. Recall that the values,  $\alpha$ , obtained in the present study are very close to MD results for Ni and Cu. That is, the difference of  $\alpha$  between the two methods is within 10%. For all the metals, the difference of  $\alpha$  between the present simulation and the experimental results is within 30%.

Table 3 shows the values of  $\alpha$ ,  $a_0$ , and  $E_c$  for Ni and Cu as computed with the Cleri potential which extends to fifth neighbors. The MD results<sup>17)</sup> and experimental data are also shown.

Although  $\alpha$  of Cu is in agreement with molecular dynamics simulation result within 20%, that of Ni is as twice as that of MD result. For  $a_0$  and  $E_c$ , there is a large discrepancy between the renormalizations and MD results. This indicates that large-ranged potentials are less suited for the potential renormalization scheme with the currently used approximations.

#### 4. Summary

The thermodynamic properties of transition metals and noble metals are studied by using a face-centered cubic (FCC) lattice model with the renormalized Rosato potential and renormalized Cleri potential. The lattice model well reproduces the linear thermal expansion coefficients,  $\alpha$ , as compared with the results of MD simulations and experiments, especially in the case of Rosato potential, whose cut-off radius is restricted to the first neighbor distance. The lattice constant at 0 K,  $a_0$ , and the cohesive energy at 0 K,  $E_c$ , are also estimated, and agree well with the corresponding MD simulations.

Spatially more extended potentials are less suitable for applying the present potential renormalization scheme.

#### Acknowledgements

The authors are grateful to the Computer Science Group of

the IMR, Tohoku University and Computer Center of Tohoku University and for their continuous support of their computing systems.

#### REFERENCES

- 1) T. Horiuchi, S. Takizawa, T. Suzuki and T. Mohri: *Metall. Mater. Trans. A* **26A** (1995) 11–19.
- 2) K. Masuda-Jindo, Vu Van Hung and Pham Dinh Tam: *Phys. Rev. B* **67** (2003) 094301.
- 3) K. Ohno: *The Sci. Rep. Res. Inst. Tohoku Univ. A* **43** (1997) 17–21.
- 4) K. Ohno, K. Esfarjani and Y. Kawazoe: *Introduction to Computational Materials Sciences: From Ab Initio to Monte Carlo Methods*, Solid-State Sciences, (Springer-Verlag, Berlin, Heidelberg, 1999) 188–197.
- 5) R. Sahara, H. Mizuseki, K. Ohno, S. Uda, T. Fukuda and Y. Kawazoe: *J. Chem. Phys.* **110** (1999) 9608–9617.
- 6) R. Sahara, H. Mizuseki, K. Ohno, H. Kubo and Y. Kawazoe: *J. Cryst. Growth* **229** (2001) 610–614.
- 7) J. Tersoff: *Phys. Rev. B* **38** (1998) 9902–9905.
- 8) H. Ichikawa, R. Sahara, H. Mizuseki, K. Ohno and Y. Kawazoe: *Mater. Trans. JIM* **40** (1999) 911–914.
- 9) R. Sahara, H. Ichikawa, H. Mizuseki, K. Ohno, H. Kubo and Y. Kawazoe: *J. Chem. Phys.* (2004) 9297–9301.
- 10) M. W. Finnis and J. E. Sinclair: *Philos. Mag. A* **50** (1984) 45–55.
- 11) G. J. Ackland and V. Vitek: *Phys. Rev. B* **41** (1990) 10324–10333.
- 12) G. J. Ackland, G. Tichy, V. Vitek and M. W. Finnis: *Philos. Mag. A* **56** (1987) 735–756.
- 13) Hui-fang Deng and David J. Bacon: *Phys. Rev. B* **48** (1993) 10022–10030.
- 14) F. Ducastelle and F. Cyrot-Lackmann: *J. Phys. Chem. Solids* **31** (1970) 1295–1306.
- 15) D. Tomanek, A. A. Aligia and C. A. Balseiro: *Phys. Rev. B* **32** (1985) 5051–5056.
- 16) V. Rosato, M. Guillope and B. Legrand: *Philos. Mag. A* **59** (1989) 321–336.
- 17) F. Cleri and V. Rosato: *Phys. Rev. B* **48** (1993) 22–33.
- 18) *Thermal Expansion: Metallic Elements and Alloys, Thermophysical Properties of Metal*, ed. by Y. S. Touloukian *et al.*, Vol. 12 (IFI/PLENUM, New York, 1972) 2–400.